NIH Public Access
Author Manuscript
J Pept Res. Author manuscript; available in PMC 2006 May 19.

Published in final edited form as:
J Pept Res. 2004 February ; 63(2): 69–84.

Effects of single D-amino acid substitutions on disruption of β-sheet structure and hydrophobicity in cyclic 14-residue antimicrobial peptide analogs related to gramicidin S

D.L. Lee, **J.-P.S. Powers**, **K. Pflegerl**, **M.L. Vasil**, **R.E.W. Hancock**, and **R.S. Hodges**

D.L. Lee, Department of Biochemistry, University of Alberta, Edmonton T6G 2H7, Canada.

J.-P.S. Powers and R.E.W. Hancock, Department of Microbiology, University of British Columbia, Vancouver, British Columbia V6T 1Z3, Canada.

K. Pflegerl, Institute of Applied Microbiology, University of Agricultural Sciences, Vienna A-1190, Austria.

M.L. Vasil, Department of Microbiology, University of Colorado Health Sciences Center, Denver, CO 80262, USA.

D.L. Lee and R.S. Hodges, Department of Biochemistry and Molecular Genetics, University of Colorado Health Sciences Center, Denver, CO 80262, USA.

Abstract

Gramicidin S (GS) is a 10-residue cyclic β-sheet peptide with lytic activity against the membranes of both microbial and human cells, i.e. it possesses little to no biologic specificity for either cell type. Structure–activity studies of de novo-designed 14-residue cyclic peptides based on GS have previously shown that higher specificity against microbial membranes, i.e. a high therapeutic index (TI), can be achieved by the replacement of a single L-amino acid with its corresponding D-enantiomer [Kondejewski, L.H. et al. (1999) *J. Biol. Chem.* **274**, 13181]. The diastereomer with a D-Lys substituted at position 4 caused the greatest improvement in specificity vs. other L to D substitutions within the cyclic 14-residue peptide GS14, through a combination of decreased peptide amphipathicity and disrupted β-sheet structure in aqueous conditions [McInnes, C. et al. (2000) *J. Biol. Chem.* **275**, 14287]. Based on this information, we have created a series of peptide diastereomers substituted only at position 4 by a D- or L-amino acid (Leu, Phe, Tyr, Asn, Lys, and achiral Gly). The amino acids chosen in this study represent a range of hydrophobicities/hydrophilicities as a subset of the 20 naturally occurring amino acids. While the D- and L-substitutions of Leu, Phe, and Tyr all resulted in strong hemolytic activity, the substitutions of hydrophilic D-amino acids D-Lys and D-Asn in GS14 at position 4 resulted in weaker hemolytic activity than in the L-diastereomers, which demonstrated strong hemolysis. All of the L-substitutions also resulted in poor antimicrobial activity and an extremely low TI, while the antimicrobial activity of the D-substituted peptides tended to improve based on the hydrophilicity of the residue. D-Lys was the most polar and most efficacious substitution, resulting in the highest TI. Interestingly, the hydrophobic D-amino acid substitutions had superior antimicrobial activity vs. the L-enantiomers although substitution of a hydrophobic D-amino acid increases the nonpolar face hydrophobicity. These results further support the role of hydrophobicity of the nonpolar face as a major influence on microbial specificity, but also highlights the importance of a disrupted β-sheet structure on antimicrobial activity.

Correspondence to: *Robert S. Hodges*, Department of Biochemistry and Molecular Genetics, University of Colorado Health Sciences Center, Denver, CO 80262 USA, Tel.: +1-303-315-8837, Fax: +1-303-315-1153, E-mail: robert.hodges@uchsc.edu

NIH-PA Author Manuscript
NIH-PA Author Manuscript
NIH-PA Author Manuscript

NIH-PA Author Manuscript

NIH-PA Author Manuscript

NIH-PA Author Manuscript

Keywords

D-amino acids; antimicrobial peptides; cationic peptides; cyclic peptides; gramicidin S; peptide diastereomers; β-sheet; structure—activity relationship

Abbreviations

Boc, N^{α} tert-butyloxycarbonyl; BOP, benzotriazol-1-yloxytris(dimethylamino)phosphonium hexafluorophosphate; BSA, bovine serum albumin; CD, circular dichroism; CMBT, 5-chloro-2-mercaptobenzothiazole; DCM, dichloromethane; DIEA, *N*,*N*-diisopropylethylamine; DMF, dimethylformamide; $diSC_3(5)$, 3,3′-dipropylthiadicarbocyanine iodide; EDT, ethanedithiol; GS, gramicidin S; GS14, a de novo designed 14-residue cyclic peptide related to GS; HBTU, 2-(1H-benzotriazole-1-yl)-1,1,3,3 tetramethyluronium hexafluorophosphate; HOBt, *N*-hydroxybenzotriazole; LPS, lipopolysaccharide; MALDI-MS, matrix-assisted laser desorption ionization mass spectrometry; MHB, Mueller Hinton broth; MIC, minimal inhibitory concentration; NMP, 1-methyl-2-pyrrolidinone; NPN, *N*-phenyl-1-napthylamine; PAM, 4-hydroxymethylphenylacetamidomethyl; RP-HPLC, reversed-phase high-performance liquid chromatography; SPPS, solid-phase peptide synthesis; TFA, trifluoroacetic acid; TFE, trifluoroethanol; TI, therapeutic index

The problem of pathogens that are becoming resistant to conventional antibiotics has emerged as a prominent global health concern, as the number of resistant bacterial strains has increased significantly in the last decades (1). The issue has brought attention to the need for alternative antimicrobial agents that bacteria have not or are unlikely to develop resistance mechanisms against. In the past two decades, a number of naturally occurring cationic antimicrobial peptides have been identified and characterized in a wide range of organisms (2–5). In contrast with conventional antibiotics that specifically inhibit essential molecules such as enzymes involved in cell wall synthesis, transcription or translation, these peptides are thought to directly interact with and disrupt the stability of the microbial membrane (6). Therefore, killing is rapid (minutes vs. hours or days) fairly nonspecific (active against a broad spectrum of gram-positive and gram-negative bacteria) and does not produce bacteria resistant to this mode of action (7).

Gramicidin S (GS) is an antimicrobial peptide that has been the subject of numerous structure–activity studies (2–12). It is active against both gram-negative and gram-positive bacteria (13), but has had limited applications as a therapeutic antimicrobial agent because of its high toxicity to human cells. GS is a cyclic 10-residue β-sheet peptide sharing features common to many antimicrobial peptides, including an overall positive (+2) charge, secondary structure in the membrane, and some degree of amphipathicity (nonpolar and polar faces). Recently, efforts have been made to design peptides related to GS that increase specificity toward microbial cells vs. mammalian cells, based on the differences in membrane lipid composition between microbial cells and human cells. Attempts have been made to dissociate antimicrobial activity from hemolytic activity by changing parameters such as ring size, β-sheet structure, and amphipathicity (9,10,14). GS analogs of four to 14 amino acids were prepared and tested for biologic activity. Although a de novo-designed peptide, GS14, enabled dissociation between antimicrobial activity and hemolytic activity, the result [poor antimicrobial activity and strong hemolytic activity, i.e. a low therapeutic index (TI)] was opposite to that desired (10). Nevertheless, the study demonstrated that it was possible to alter membrane specificity between microbial and human cells by sequence manipulation. In a subsequent study of GS14 analogs, introducing D-enantiomers in the ten β-strand positions that normally contain L-amino acids reversed this activity profile. These GS14 diastereomers had disrupted β-sheet structure in benign medium and reduced amphipathicity due to positioning of the D-amino acid side-chain

NIH-PA Author Manuscript

NIH-PA Author Manuscript

NIH-PA Author Manuscript

on the opposite face of the molecule compared with the L-counterpart. Inversion of the optical center of the amino acid substitution resulted in nonpolar amino acids on the polar face and polar amino acids on the nonpolar face, while maintaining the same overall hydrophobicity as GS14. The peptide with the highest TI (hemolytic activity/antimicrobial activity) was a GS14 diastereomer with D-Lys substituted at position 4 (GS14K4) (14).

In this study, we continue to investigate the effects of enantiomeric substitutions in GS14. Here, we substitute single D-amino acids specifically at position 4 that span a wide range of side-chain hydrophobicities. These substitutions, in addition to disrupting β-sheet structure and affecting amphipathicity, also change the overall peptide hydrophobicity. Moreover, to determine which of these parameters are responsible for the changes in biologic activity, we also studied GS14 peptides with the corresponding L-amino acid at position 4 to compare differences in structure, amphipathicity and activity between D- and L-diastereomers. In addition, we substituted the achiral amino acid glycine at position 4 to examine its effect on disruption of β-sheet structure and biologic activity in the absence of a side-chain. We find here that all L-substituted peptides maintained a β-sheet structure, and generally have strong hemolytic activity and weak antimicrobial activity. Although the Gly substitution disrupted β-sheet structure, it did not significantly improve hemolytic or antimicrobial activity over the L-substitutions. The D-substitutions disrupted β-sheet structure, with varying improvements in hemolytic and antimicrobial activity. Polar D-substitutions provided the best improvements in TI, with the D-Lys substituted peptide yielding the highest therapeutic indices in this study against all microorganisms tested. These results support the hypothesis that an optimal nonpolar face hydrophobicity coupled with a disrupted β-sheet structure can maximize microbial specificity in the GS14 cyclic β-sheet structural template.

Materials and Methods

Microbial strains

Strains used in the antimicrobial assays include the yeast *Candida albicans;* gram-negative bacteria including the antibiotic-sensitive mutant *Salmonella typhimurium* C610, *Escherichia coli* UB1005 and its antibiotic-sensitive mutant DC2; and gram-positive bacteria including wild-type and methicillin-resistant (SAP0017) strains of *Staphylococcus aureus* and an environmental isolate of *Bacillus subtilis.*

Materials

All microbial strains were grown on Mueller Hinton broth (MHB) for antibacterial assays (Difco Laboratories, Detroit, MI, USA). N^{α} *tert*-butyloxycarbonyl (Boc)-Pro-4-hydroxymethylphenylacetamidomethyl (PAM) resin, benzotriazol-1-yloxytris (dimethylamino)phosphonium hexafluorophosphate (BOP), 2-(1H-benzotriazole-1-yl)-1,1,3,3 tetramethyluronium hexafluorophosphate (HBTU), *N*-hydroxybenzotriazole (HOBt), and Boc amino acids were from NovaBiochem (La Jolla, CA, USA), with the exception of Boc-Lys(formyl)-OH from Bachem (Torrance, CA, USA). Trifluoroacetic acid (TFA) was from Halocarbon (River Edge, NJ, USA). Anisole, ethanedithiol (EDT), *N*,*N*-diisopropylethylamine (DIEA), and ninhydrin were from Sigma Chemical Co. (St Louis, MO, USA). Phenol, ethyl ether, hydrochloric acid, ethanol, acetonitrile, methanol, dichloromethane (DCM), and dimethylformamide (DMF) were from Fisher Scientific (Fairlawn, NJ, USA).

Peptide synthesis, purification, and cyclization

Peptides were synthesized by the solid-phase method with Boc-amino acids, as described previously (10). Briefly, Boc--Pro-PAM resin (0.1 mmol) was used as the starting material. Resin was deprotected 15 min with 50% TFA in DCM to remove the Boc group from the α-amino group, neutralized with 5% DIEA in DCM, and coupled with 0.4 mmol of Boc-amino

NIH-PA Author Manuscript

NIH-PA Author Manuscript

NIH-PA Author Manuscript

acid activated with equimolar amounts of HBTU and HOBt and a 1.2 m excess of DIEA. Couplings were monitored for completion by a qualitative ninhydrin test. Peptides were cleaved from resin with a cocktail of anhydrous HF/anisole/EDT (10:0.5:0.02), at 4 °C for 1 h. Cleavage cocktail was removed under reduced pressure, and the peptide-resin was washed with cold diethyl ether, extracted with 60% aqueous acetonitrile, and lyophilized to dry powder. Linear crude peptides were purified on a Beckman System Gold HPLC (Beckman Instruments, Berkeley, CA, USA), using a Brownlee Aquapore RP-300 column, 250 × 7.0 mm ID (Brownlee Labs, Santa Clara, CA, USA). Peptides were eluted in a 20–60% B linear gradient, 2 mL/min, at 0.25% B/min, where A = 0.05% aqueous TFA, B = 0.05% TFA in acetonitrile. Elution profiles were monitored at 280 nm. Peak purity was verified by matrix-assisted laser desorption ionization mass spectrometry (MALDI-MS) using a 5-chloro-2-mercaptobenzothiazole (CMBT) matrix, and analytical reversed-phase HPLC (RP-HPLC). Pure linear peptides were cyclized with 5 eq. DIEA, 3 eq. HBTU and 3 eq. HOBt in DMF at 2 mg/mL peptide concentration. The cyclization reaction was complete after 1 h. DMF was removed by rotary evaporation, and the mixture was deformylated in 20% HCl in methanol at 40 °C for 12 h. Solvent was removed by rotary evaporation, and the peptide was solubilized in aqueous acetonitrile (up to 40% depending on peptide solubility) for HPLC purification. Cyclized peptides were purified on a 0.25% B/min linear gradient, 2 mL/min, with the starting and ending compositions dependent on peptide solubility (elution conditions ranged from 20 to 70% B) and purified fractions were lyophilized to a dry powder.

Circular dichroism spectroscopy

Circular dichroism (CD) scans were performed as described previously (10). Briefly, scans were obtained on a Jasco J-720 Spectrapolarimeter (Jasco, Easton, MD, USA) using a 0.2 cm quartz cuvette. An average of five to eight scans were collected between 190 and 255 nm at 100 nm/min for 20 μM peptide solutions in either 5 mM sodium acetate, pH 5.5 or 5 mM sodium acetate, 50% trifluoroethanol (TFE), pH 5.5. Concentrations of peptide stock solutions were determined by amino acid analysis.

Minimal inhibitory concentration assays

Antibacterial assays were performed using the modified microtiter dilution method for cationic antimicrobial peptides, as described by Hancock et al. (http://cmdr.ubc.ca/bobh/MIC.htm). Bacteria were grown overnight at 37 °C and diluted in MHB to give 2–7 × 10^5 colony forming units/mL. Peptides were dissolved and diluted in 0.01% acetic acid, 0.2% bovine serum albumin (BSA). Bacterial aliquots of 100 μL were incubated 18–24 h at 37 °C with 11 μL peptide (2–96 mg/mL final concentration) in MHB. Minimal inhibitory concentration (MIC) was defined as the minimal peptide concentration required to inhibit bacterial growth by at least 50%.

Hemolysis assays

The hemolytic activity for each peptide was determined by making twofold serial dilutions of the peptide sample in a microtiter plate to a final volume of 100 μL, and adding 100 μL of washed human erythrocytes (RBC) in a 1% suspension based on packed cell volume. Concentrations of peptide stock solutions were determined by amino acid analysis. Plates were incubated for 2 or 24 h at 37 °C and the minimal peptide concentration for complete RBC lysis was considered to be the hemolytic activity for that peptide, reported in μg/mL (except in Fig. 5). The hemolytic activity bar graph in Fig. 5 is displayed in reciprocal units, $(\mu g/mL)^{-1}$, for the purpose of using high values to show the peptides with strong hemolytic activity (in contrast with the values reported in μg/mL, which are inversely proportional to activity). There was never greater than a twofold change in activity for any peptide from 2 to 24 h. A negative control was determined from samples of 200 μL of 1% RBC with no peptide present.

NIH-PA Author Manuscript

NIH-PA Author Manuscript

NIH-PA Author Manuscript

Analytical HPLC

Runs were performed on a Hewlett Packard 1100 chromatograph using a Zorbax 300 SB C_8 column (15 × 0.2 cm ID, 5 μm particle size, 300 Å pore size; Rockland Technologies, Wilmington, DE, USA). Elution was from 0 to 70% B, 1% B/min gradient rate, 0.3 mL/min flow rate, where A = 0.05% aqueous TFA and B = 0.05% TFA in acetonitrile. Peaks were detected by absorbance at 210 nm.

Permeabilization of outer membranes to *N*-phenyl-1-napthylamine

The ability of peptides to increase outer membrane permeability of gram-negative bacteria was determined by measuring incorporation of the fluorescent dye *N*-phenyl-1-napthylamine (NPN) into the outer membrane of *E. coli* UB1005 (15). Permeabilization studies were carried out as described previously (16,17). Briefly, *E. coli* UB1005 cells were suspended in 5 mM sodium HEPES buffer, pH 7.0, containing 5 mM glucose and 5 mM carbonyl cyanide *m*-chlorophenylhydrazone. NPN was added to 2 mL of cells in a quartz cuvette to give a final concentration of 10 μM and the background fluorescence recorded (excitation λ 350 nm, emission λ 420 nm). Aliquots of peptide were added to the cuvette and fluorescence recorded as a function of time until there was no further increase in fluorescence.

As outer membrane permeability is increased by addition of peptide, NPN incorporated into the membrane causes an increase in fluorescence. Values were converted to % NPN uptake using the equation

$$\%\ \text{NPN uptake} = (F_{obs} - F_0) / (F_{100} - F_0) \times 100$$

where F_{obs} is the observed fluorescence at a given peptide concentration, F_0 the initial fluorescence of NPN with *E. coli* cells in the absence of peptide, and F_{100} is the fluorescence of NPN with *E. coli* cells upon addition of 10 μg/mL polymyxin B, which is used as a positive control in this assay because of its strong outer membrane permeabilizing properties (18).

3,3′-Dipropylthiadicarbocyanine iodide release assay

To measure the ability of peptides to disrupt the electrochemical potential across the bacterial cytoplasmic membrane, the release of the membrane-associated probe, 3,3′-dipropylthiadicarbocyanine iodide [diSC$_3$(5)], from *E. coli* DC2 cells was monitored by fluorescence spectroscopy as described previously (19). Fluorescence of the dye is quenched upon initial incorporation into the cytoplasmic membrane; as peptide is added, the membrane is depolarized (inside becomes less negative) and the dye is released into the aqueous medium, resulting in increased fluorescence (20). The *E. coli* mutant DC2 strain was used because its increased outer membrane permeability allows the dye to be incorporated into the inner cytoplasmic membrane. Luria broth was inoculated with an overnight culture of cells, grown at 37 °C to mid-logarithmic phase (OD_{600}, 0.5–0.6) and pelleted in a centrifuge. The cells were washed with 5 mM HEPES, pH 7.2, 5 mM glucose buffer and resuspended in the same buffer to OD_{600} ~0.05. Addition of aliquots of 0.4 μm diSC$_3$(5) was monitored at 670 nm until reduction of fluorescence due to quenching was maximal. Potassium chloride was added to a final concentration of 100 mM to equilibrate the cytoplasmic and external K^+ concentrations. Suspensions of 2 mL were added to a 1 cm quartz cuvette and the fluorescence was continuously monitored (excitation λ 622 nm, emission λ 670 nm) upon addition of peptide on a Perkin-Elmer model LS-50B (Perkin Elmer Life and Analytical Sciences, Boston, MA, USA).

NIH-PA Author Manuscript

NIH-PA Author Manuscript

NIH-PA Author Manuscript

Results

Peptide design

The peptide sequences used in this study were based on the GS14 sequence (10), with amino acids substituted at position 4 (Fig. 1). GS14 is a cyclic β-sheet peptide possessing high amphipathicity, i.e. nonpolar and polar residues are distributed on opposite faces of the molecule (Fig. 2, left) (21). Although GS14 exhibited strong hemolytic activity and weak antimicrobial activity, diastereomers with D-amino acid substitutions at various ring positions disrupted β-sheet structure and decreased amphipathicity, resulting in weaker hemolytic activity and stronger antimicrobial activity, i.e. a higher TI (14). Notably, the GS14 diastereomer with D-Lys at position 4 had the highest TI ($GS14K_d4$; Figs 1 and 2) compared with enantiomeric substitutions at other positions in the two strands of the β-sheet. For this reason, we chose to study position 4 diastereomers, substituting D-amino acids covering a broad range of hydrophobicities, to compare structure–activity relationships. If the $GS14X_d4$ diastereomers in this study are structurally similar to $GS14K_d4$ (as we anticipate with a constrained head-to-tail cyclic peptide), the substituted D-amino acids should be positioned on the nonpolar face, disrupt β-sheet structure, and alter both amphipathicity and hydrophobicity of the nonpolar face (Fig. 2, right). Furthermore, we predict that $GS14X_l4$ peptides, although differing in hydrophobicity and amphipathicity, will remain β-sheet in a manner consistent with the GS14 structure. In this study, we present data for six amino acid substitutions at position 4 (a total of 11 peptides: five $GS14X_l4$, five $GS14X_d4$, and GS14G4) representing a range of hydrophobicities found among the twenty amino acids. The substitutions include Gly (no side-chain), Lys (polar charged), Asn (polar), Tyr and Phe (aromatic) and Leu (large aliphatic hydrophobe). Our main objective in this study was to investigate the role of the hydrophobicity of D-amino acid substitutions at position 4 of GS14 on biologic specificity between microbial cells and human cells.

Circular dichroism spectroscopy

We examined secondary structures of GS14X4 peptides in benign and membrane-mimicking solvents (see Materials and Methods). $GS14X_l4$ peptides form β-sheet structures in benign conditions, as shown by their CD spectra with local minima at 205 and 220 nm (Fig. 3A). The spectra of these peptides are not characteristic of conventional β-sheet spectra due to the major contribution of the type II′ β-turns to molar ellipticity at ~205 nm, and appear similar to the representative spectrum of an α-helix (14); therefore, an estimate of per cent β-sheet could not be calculated. In addition, the aromatic amino acid tyrosine, present in all peptide analogs in this study, influences the far-UV CD spectra (22–24). However, the NMR solution structures of GS14 and $GS14K_d4$ have previously been determined (21) and show the respective β-sheet and disrupted β-sheet conformations that correspond to the helix-like CD spectra of these peptides.

In 50% TFE, the $GS14X_l4$ peptides became more structured, as indicated by the increase in negative molar ellipticity observed, e.g. in $GS14L_l4$ (Fig. 3A; Table 1). The Gly substituted GS14G4 went from a disrupted β-sheet in benign solution (maxima shifted from 205 to ~202 nm and decreased negative molar ellipticity at 220 nm vs. $GS14L_l4$ spectrum; Fig. 3A) to a more ordered structure in TFE (Fig. 3B). Similarly, the D-substitutions also disrupted β-sheet structure in benign medium and formed a more ordered structure in TFE. In TFE, $[\theta]_{220}$ values were generally similar for L- and D-diastereomers and GS14G4 ranging from −34 000 to −27 800, with the exception of D-Asn at −23 400. The extent of inducible structure ($\Delta [\theta]_{220}$ TFE−benign) (Table 1) was greater for some D-diastereomers vs. L-diastereomers because the $GS14X_d4$ peptides were less structured in benign conditions. The achiral Gly substituted peptide showed inducibility (−11 300) intermediate between D- and L-diastereomers and its $[\theta]_{220}$ value in benign solvent (−18 400) was also intermediate between values of D- and L-

NIH-PA Author Manuscript

NIH-PA Author Manuscript

NIH-PA Author Manuscript

substituted peptides. There appeared to be no correlation between hydrophobicity of the substituted D-amino and the extent of inducible structure. For example, both GS14K_d4 and GS14L_d4 exhibited a disrupted structure in benign medium and large inducibility in 50% TFE (Table 1), although they are at opposite extremes of the amino acid hydrophobicity scale (25).

Analytical HPLC

Reversed-phase HPLC is commonly employed to resolve molecules based on differences in overall inherent hydrophobicity, i.e. the hydrophobicity determined by a protein or peptide primary amino acid sequence. But the technique can also separate molecules with identical overall inherent hydrophobicites that differ only in hydrophobicity at the preferred binding domain (nonpolar face) of an amphipathic molecule. For example, in addition to achieving separation for peptides with different intrinsic hydrophobicities, e.g. those within the GS14X_l4 or GS14X_d4 series (Fig. 4), we also observed different retention times between D- and L-diastereomers with the same inherent hydrophobicities (Table 2). The results suggest that the GS14X_d4 peptides indeed have their D-side-chains positioned on the nonpolar face. Figure 4 shows that there is a very broad range of retention times for D-diastereomers (18.1 min) vs. L-diastereomers (3.5 min). Presumably, this is because the D-amino acids are positioned on the GS14 nonpolar face, which forms the preferred binding domain that provides the major interaction with the hydrophobic column matrix to determine peptide retention time. The NMR solution structure of GS14K_d4 shows the D-Lys side-chain on the nonpolar face, and we assume that the positioning is similar with other D-substitutions in GS14X_d4 peptides (21). Polar D-substitutions such as D-Asn and D-Lys change the hydrophobicity of the preferred binding domain the most, thus decreasing retention time. In contrast, peptides substituted with L-Leu, L-Tyr and L-Asn were not resolved although the intrinsic hydrophobicity of these side-chains are enormously different. The hydrophobicity of the substituted D-amino acid thus determines the relative retention time of the D-diastereomer, while substituted L-amino acids (on the GS14 polar face) have little effect on peptide retention time.

In comparing retention times between GS14X_l4 and GS14X_d4 peptides, those that were more retentive than their respective diastereomers were consistent with sequences possessing a higher amphipathic character, i.e. containing either nonpolar D-substitutions on the nonpolar face, or polar L-substitutions on the polar face (Table 2). Within the GS14X_d4 series, peptides eluted in an order generally consistent with previous hydrophobicity scales obtained by RP-HPLC (25,26) and scales derived from non-HPLC techniques (27,28). In summary, peptides used in this study have a broad range of intrinsic hydrophobicities and amphipathicities, as indicated by examination of their sequences, with RP-HPLC separation achieved through differences in one or both of these parameters.

Hemolytic activity

All L-diastereomers and GS14G4 were strongly hemolytic (Table 3). D-diastereomers were generally less hemolytic when the substituted amino acid was very polar (D-Asn and D-Lys), with GS14K_d4 being the most polar and the least hemolytic peptide in this study (Fig. 5). Hemolytic activity was strong for both D- and L-substitutions with the nonpolar amino acids Leu and Phe, likely because these amino acids did not reduce the hydrophobicity of the nonpolar face (Fig. 4, top) and, in the case of D-Phe and D-Leu, actually increased it. Although GS14G4 exhibited a disrupted β-sheet structure in benign medium, the Gly substitution did not reduce the hydrophobicity of the nonpolar face and also did not weaken hemolytic activity. Although the killing mechanism of these peptides has not been determined, the high hydrophobicity of the nonpolar face may increase specificity toward mammalian membranes through interactions between peptide and uncharged lipids found only in eukaryotic cells, such as cholesterol (29,30).

NIH-PA Author Manuscript

NIH-PA Author Manuscript

NIH-PA Author Manuscript

Antimicrobial activity

L-Diastereomers were, in general, considerably less active against all microorganisms assayed vs. their D-counterparts (Tables 3 and 4). GS14G4 also exhibited poor antimicrobial activity on par with the $GS14X_l4$ peptide. D-Diastereomers had more complicated patterns for activity, and did not display a simple dependence on polarity of the substituted amino acid, in contrast with hemolysis results (Fig. 5). It is important to note that hemolytic activity and antimicrobial activity are shown in Fig. 5 in reciprocal units, to allow facile comparisons between hemolytic activity, antimicrobial activity and TI (higher values always correspond to higher activities). Between gram-positive bacteria, gram-negative bacteria, and yeast, the antimicrobial activity of $GS14X_d4$ peptides was generally stronger against gram-positive bacteria (see $GS14Y_d4$ results; Fig. 5). Although $GS14X_d4$ peptides with nonpolar substitutions displayed some antimicrobial activity, the most active peptide against gram-positive bacteria and yeast ($GS14Y_d4$) and the most active against gram-negative bacteria ($GS14K_d4$) both contained polar substitutions (Fig. 5). $GS14Y_d4$ was the most active peptide against six strains tested (four gram-positive, one yeast and one gram-negative) and was second-most active in the other two gram-negative strains.

Therapeutic index

Peptides with a consistently poor TI (<1) against all microbial strains tested were the L-diastereomers in the $GS14X_l4$ series, as well as peptides substituted with Gly, D-Phe, and D-Leu (Tables 3 and 4). In the $GS14X_d4$ series, the value of TI vs. gram-negative organisms increases with increasing polarity of the D-substitution (as measured by RP-HPLC retention time; Fig. 6), but there is no obvious relationship between TI and peptide hydrophobicity in gram-positive bacteria (Fig. 5).

The peptide with the best TI against gram-negative bacteria and yeast was $GS14K_d4$ (Fig. 6; Table 3). We observed both improved antimicrobial activity vs. gram-negative bacteria and decreased hemolytic activity for $GS14K_d4$ compared with its diastereomer, GS14 (Table 3; Fig. 5). Interestingly, against gram-positive bacteria, $GS14K_d4$ also had the best TI, although overall TI values were lower compared with TI vs. gram-negative bacteria because there was little or no improvement in antimicrobial activity for $GS14K_d4$ compared with GS14 for gram-positive bacteria (maximum TI of 16 vs. 62, Tables 3 and 4).

If we turn our attention away from absolute values of TI and instead focus on relative gains in TI in switching from L- to D-diastereomers, we see that $GS14X_d4$ peptides with hydrophobic substitutions displayed little or no improvement, whereas $GS14N_d4$ (20–400-fold) and $GS14K_d4$ (40–1600-fold) were notable for their considerable improvement in activity over their L-diastereomers (Tables 3 and 4). $GS14N_d4$ showed a gain in TI over its diastereomer primarily because it had weaker hemolytic activity, $GS14Y_d4$ improved TI because of its stronger antimicrobial activity, and $GS14K_d4$ showed the best improvement by favorably altering both antimicrobial and hemolytic activity. Therefore, in this study polar D-enantiomeric substitutions improved TI in various combinations, by affecting one ($GS14Y_d4$, $GS14N_d4$) or both ($GS14K_d4$) of the antimicrobial and hemolytic activities.

Peptide–lipid interactions

Peptides were evaluated for their ability to interact with membranes and membrane components in the fluorescence-based NPN uptake and $diSC_3(5)$ release assays (see Materials and Methods). While the NPN uptake studies showed peptide permeabilizing effects on the outer membrane of gram-negative bacteria (Fig. 7), the $diSC_3(5)$ release assay indicated the peptides ability to disrupt the membrane potential across the inner cytoplasmic membrane (Fig. 8).

NIH-PA Author Manuscript

NIH-PA Author Manuscript

NIH-PA Author Manuscript

The NPN uptake results showed that all of the peptides except GS14N$_l$4 were able to permeabilize the outer membrane to a similar degree (Fig. 7). The greatest difference in permeability was between L- and D-Asn substituted peptides, because addition of the L-Asn peptide appeared to cause cells to aggregate in the cuvette, preventing the complete uptake of NPN. GS14N$_l$4 possibly induced cellular aggregation due to intermolecular hydrogen bonding between Asn side-chains on the polar faces of adjacent peptides that might have contributed to cell aggregation.

Although there were few differences between D- and L-diastereomers in increasing outer membrane permeability, we observed more differences in diastereomers influencing the permeability of the cytoplasmic membrane. In the diSC$_3$(5) assay, all of the D-diastereomers except GS14-K$_d$4 released more dye than GS14G4 at their respective MIC concentrations, while all of the L-diastereomers released less dye than GS14G4, indicating that the D-diastereomers were generally more disruptive to the cytoplasmic membrane potential than the L-diastereomers (Fig. 8). The D-diastereomers also showed a broader range of ability to depolarize the cytoplasmic membrane over the L-diastereomers, which all exhibited similar weakly depolarizing behavior. These results may suggest that the conserved β-sheet structure among the L-diastereomers somehow decreases the extent of cytoplasmic membrane depolarization relative to the disrupted β-sheet structure of the D-diastereomers. Among the peptides substituted with D-amino acids, the most disruptive peptide was GS14F$_d$4 (D-Phe substitution), one of the most hydrophobic peptides in this study (Fig. 4), while the weakest was GS14K$_d$4, which also exhibited the best antimicrobial activity against the outer-membrane permeable *E. coli* DC2 cells used in the diSC$_3$(5) assay (Table 3). Although poor cytoplasmic membrane depolarization ability is not correlated with either strong or weak antimicrobial activity in this study, the results for GS14K$_d$4 suggest that the ability to depolarize the cytoplasmic membrane is not a requirement for strong antimicrobial activity.

Discussion

Our main objective in this study was to investigate the role of the D- and L-amino acid substitutions at position 4 of GS14 on specificity between microbial cells and human cells. The substitution of single D-amino acids at position 4 change the side-chain stereochemistry, which in turn can affect three parameters of the peptide to varying degrees: overall hydrophobicity, amphipathicity, and the degree of secondary (β-sheet) structure in benign medium.

Overall inherent hydrophobicity

Previous studies have shown that for antimicrobial peptides in various structural categories, the hydrophobicity of the peptide must exceed a minimal value to exert antimicrobial and hemolytic activity. The differences between this minimal hydrophobicity value for microbial cells and human cells provide a window that allows the development of peptides with selectivity toward microbial membranes (31). However, as hydrophobicity increases beyond a certain value, selectivity is lost as peptides become both strongly hemolytic and strongly antimicrobial (31,32). Dramatic differences in biologic activity observed between peptide diastereomers in this study indicate that overall inherent hydrophobicity (identical in both L- and D-diastereomers) is less important than the hydrophobicity of the nonpolar face of the molecule (altered only in the D-diastereomers) in modulating microbial specificity. For example, the range of inherent hydrophobicities in substituting L-amino acids (Lys, Asn, Tyr, Phe, and Leu) at position 4 is large, yet there was little effect on hemolytic activity. Using the hydrophobicity scale of Sereda *et al.* (25), the coefficients for these amino acid side-chains are −3.14, −3.46, 4.16, 7.86, and 8.50, respectively. Similarly, other hydrophobicity scales show the same dramatic differences in the hydrophobicity of these residues [see review by Liu and Deber (33) and references therein]. All of the GS14X$_l$4 peptides in this study had similar and

NIH-PA Author Manuscript

NIH-PA Author Manuscript

NIH-PA Author Manuscript

strong hemolytic activity as the L-substitutions did not affect the hydrophobicity of the nonpolar face, as shown by RP-HPLC results where the L-analogs had similar retention times (Fig. 4).

Amphipathicity

Amphipathicity is a known requirement for antimicrobial activity in helical peptides (34) and highly amphipathic molecules have been shown to increase specificity toward mammalian membranes. In agreement with these findings, the highly amphipathic GS14 peptide (Fig. 2) with four lysine residues on the hydrophilic face and six large hydrophobes (three Val and three Leu residues) on the hydrophobic face had reduced antimicrobial activity, and was very hemolytic (14). Interestingly, GS14K_d4 (Fig. 2) had significantly reduced amphipathicity with the D-Lys being presented on the hydrophobic face, leaving only three lysine residues on the hydrophilic face (21). This peptide had increased antimicrobial activity and reduced hemolytic activity relative to GS14. Notably, all D-analogs in this study with a hydrophilic side-chain presented on the hydrophobic face (D-Tyr, D-Asn, and D-Lys) displayed reduced amphipathicity, increased antimicrobial activity and increased TI over their L-diastereomers (Fig. 5). To further support the role of amphipathicity in biologic activity and specificity, a GS14 analog containing a sequence change from Leu^3–Lys^4 to Lys^3–Leu^4 had very similar hemolytic and antimicrobial activity profiles to GS14K_d4 (21). The switch of leucine and lysine maintains the β-sheet structure but places the L-Lys residue on the hydrophobic face and places L-Leu on the hydrophilic face to reduce amphipathicity over GS14, and significantly improves the TI over GS14.

Secondary structure

The induction of secondary structure in passing from an aqueous environment to the hydrophobic membrane environment has been observed to increase microbial specificity in helical peptides (35). We have previously observed that D-amino acid substitution in GS14, which disrupts β-sheet structure in benign medium but allows induction of structure in hydrophobic medium, serves to reduce peptide binding affinity to bacterial lipopolysaccharide, reduce amphipathicity, weaken hemolytic activity and strengthen antimicrobial activity (14). These results suggest that this change in structure from benign to hydrophobic medium is important. However, others have shown that diastereomers of helical peptides substituted with D-amino acids displayed little or no secondary structure in benign medium, and exhibited reduced hemolytic activity and retained antimicrobial activity over their L-counterparts without requiring secondary structure in a hydrophobic environment (36,37). In the same studies, preformed secondary structure in benign medium can unfavorably increase specificity for mammalian membranes. This is in contrast with the results for a cyclic β-sheet peptide which is also preformed in benign medium, yet had excellent specificity for microbial cells (21). Substitution of D-amino acids is known to be disruptive to secondary structure of linear α-helical peptides (38) and cyclic peptides (21) in benign medium, but the extent of induction in hydrophobic medium is larger in the former category. Although the extent of disruption of structure in benign medium and induction in membranes by D-amino acids is greater for linear peptides (such as melittin and pardaxin), in contrast with cyclic peptides (such as GS), we have seen that even subtle structural changes can have major effects on biologic activity in both cyclic and linear structural frameworks.

In this study, we observed that D-Phe and D-Leu substitutions both increased nonpolar face hydrophobicity, yet showed improvements in antimicrobial activity and TI over their respective L-diastereomers (Tables 3 and 4). An increase in nonpolar face hydrophobicity above that of GS14 would be expected to cause a loss of microbial specificity, with peptides becoming both more hemolytic and more antimicrobial (31). As we do not observe this result in D-Phe and D-Leu substitutions, which disrupt β-sheet structure in addition to increasing nonpolar face

NIH-PA Author Manuscript

NIH-PA Author Manuscript

NIH-PA Author Manuscript

hydrophobicity, it appears that the improved biologic activity in GS14L_d4 and GS14F_d4 peptides over their diastereomers can be attributed to the disrupted β-sheet structure.

How does the induction of secondary structure in hydrophobic environments relate to the model of peptide–lipid interactions? The mechanism of peptide-induced membrane destabilization by cyclic β-sheet peptides has been studied with the 10-residue peptide, GS, in liposomes and lipid films (39–41). Assuming that the peptide–lipid interaction mechanism for GS14 is similar to the behavior of GS (both have β-sheet structures, high amphipathicity, and similar charge per residue ratios of 2/10 = 0.2 and 4/14 = 0.286, respectively), these peptides initially exert specificity toward bacterial membranes through long-range electrostatic interactions between the anionic cell membrane and the cationic peptide, causing association at the bilayer interface. Subsequently, the peptide molecule associates parallel to the membrane (42), in the interfacial region between the polar glycerol backbone and the hydrocarbon chains, whereupon a peptide conformational change in the hydrophobic medium drives membrane association and bilayer penetration. In this study, all of the D-amino acid substitutions disrupted GS14X4 structure in benign medium and were inducible in trifluoroethanol, although it was not clear whether the inducible structure contributed to observed differences in activity or specificity. However, it is plausible that the induction of β-sheet structure is not a requirement as long as the peptide is able to traverse the bacterial lipid bilayer. The disrupted β-sheet structure may facilitate this process better than the more rigid β-sheet structure found in GS14 and the L-substituted peptide analogs in this study.

The most antimicrobial peptides in this study had D-amino acids positioned on the nonpolar face, which would likely interact with the nonpolar hydrocarbon chains in the membrane bilayer. However, only the peptides with polar D-amino acids had weakened hemolytic activity (Fig. 6). It is possible that the polar D-amino acid on the GS14 nonpolar face increases microbial specificity over the L-diastereomer by excluding the peptide from cholesterol-containing mammalian membranes. This behavior was observed in Fourier transform infrared spectroscopy studies of GS14K_d4 in lipid micelles and bilayer systems (30).

We observed that GS14K_d4 had the best TI over other peptides substituted with polar D-amino acids, including D-Asn and D-Tyr. From a molecular standpoint, the positive charge on the ε-amino group of D-lysine 4 in GS14K_d4 resulted in the greatest effect on the hydrophobicity of the nonpolar face, and a lower amphipathicity than the β-carboxamide side-chain of GS14N_d4 or the phenolic ring in GS14Y_d4. The positive charge on the D-Lys compared with other polar side-chains at position 4 may have increased specificity toward microbial membranes because of the anionic character of microbial membranes (in contrast with zwitterionic mammalian membranes), which may partially explain why GS14K_d4 displayed the strongest antimicrobial activity of all the peptides studied here against gram-negative organisms. In contrast, GS14Y_d4 had excellent antimicrobial activity vs. gram-positive bacteria, possibly because the higher hydrophobicity in the phenolic tyrosine ring (compared with the asparagine and lysine side-chain) is better suited to penetrating the peptidoglycan layer of gram-positive bacteria to interact with the cell membrane.

We have shown that for peptides utilizing the cyclic β-sheet structural framework of GS14, the substitution of polar D-enantiomers can improve TI through improvements in antimicrobial activity and/or through decreasing hemolytic activity. Exceeding a certain overall hydrophobicity causes an increased specificity for mammalian membranes and results in strong hemolytic and weak antimicrobial activity. It is conceivable that substitutions of other D-amino acids at position 4 may improve TI values more than the best peptide in this study, GS14K_d4, and lead to the development of more efficacious antimicrobial therapeutics suitable for human use.

NIH-PA Author Manuscript

NIH-PA Author Manuscript

NIH-PA Author Manuscript

Acknowledgements

We thank Marc Genest for assistance with peptide synthesis and purification, Susan Farmer for assistance with MIC assays, and Adriana Vasil for performing hemolysis assays. D.L. is funded by NSERC and the Alberta Heritage Foundation for Medical Research. M.L.V. is supported by the National Heart, Blood and Lung Institute HL62608. R.S.H. is supported by NIH RO1 grants, GM-61855 and AI48717.

References

1. Lohner, K. & Staudegger, E. (2001) Are we on the threshold of the post-antibiotic era? In: *Development of Novel Antimicrobial Agents:* Emerging Strategies (Lohner, K., ed.), pp. 1–15. Horizon Scientific Press, Wymondham.
2. Balasubramanian D. The conformation of gramicidin S in solution. J Am Chem Soc 1967;89:5445–5449. [PubMed: 6073140]
3. Conti F. 220 MHz nuclear magnetic resonance spectra of gramicidin S in solution. Nature 1969;221:777–779. [PubMed: 5775379]
4. Aarstad K, Zimmer TL, Laland SG. Replacement of phenylalanine in gramicidin S by other amino acids. FEBS Lett 1979;103:118–121. [PubMed: 89046]
5. Ando S, Aoyagi H, Shinagawa S, Nishino N, Waki M, Kato T, Izumiya N. [4,4′-D-diaminopropionic acid]gramicidin S: a synthetic gramicidin S analog with antimicrobial activity against Gram-negative bacteria. FEBS Lett 1983;161:89–92. [PubMed: 6193012]
6. Yonezawa H, Okamoto K, Tomokiyo K, Izumiya N. Mode of antibacterial action by gramicidin S. J. Biochem (Tokyo) 1986;100:1253–1259. [PubMed: 2434469]
7. Katsu T, Kobayashi H, Fujita Y. Mode of action of gramicidin S on *Escherichia coli* membrane. Biochim Biophys Acta 1986;860:608–619. [PubMed: 2427118]
8. Zidovetzki R, Banerjee U, Harrington DW, Chan SI. NMR study of the interactions of polymyxin B, gramicidin S, and valinomycin with dimyristoyllecithin bilayers. Biochemistry 1988;27:5686–5692. [PubMed: 2460131]
9. Tamaki M, Arai I, Akabori S, Muramatsu I. Role of ring size on the secondary structure and antibiotic activity of gramicidin S. Int. J Pept Protein Res 1995;45:299–302.
10. Kondejewski LH, Farmer SW, Wishart DS, Kay CM, Hancock RE, Hodges RS. Modulation of structure and antibacterial and hemolytic activity by ring size in cyclic gramicidin S analogs. J Biol Chem 1996;271:25261–25268. [PubMed: 8810288]
11. Tamaki M, Akabori S, Muramatsu I. Properties of synthetic analogs of gramicidin S containing L-serine or L-glutamic acid residue in place of L-ornithine residue. Int J Pept Protein Res 1996;47:369–375. [PubMed: 8791160]
12. Jelokhani-Niaraki M, Kondejewski LH, Farmer SW, Hancock RE, Kay CM, Hodges RS. Diastereoisomeric analogues of gramicidin S: structure, biological activity and interaction with lipid bilayers. Biochem J 2000;349:747–755. [PubMed: 10903135]
13. Kondejewski LH, Farmer SW, Wishart DS, Hancock RE, Hodges RS. Gramicidin S is active against both gram-positive and gram-negative bacteria. Int J Pept Protein Res 1996;47:460–466. [PubMed: 8836773]
14. Kondejewski LH, Jelokhani-Niaraki M, Farmer SW, Lix B, Kay CM, Sykes BD, Hancock RE, Hodges RS. Dissociation of antimicrobial and hemolytic activities in cyclic peptide diastereomers by systematic alterations in amphipathicity. J Biol Chem 1999;274:13181–13192. [PubMed: 10224074]
15. Loh B, Grant C, Hancock RE. Use of the fluorescent probe 1-N-phenylnaphthylamine to study the interactions of aminoglycoside antibiotics with the outer membrane of *Pseudomonas aeruginosa*. Antimicrob Agents Chemother 1984;26:546–551. [PubMed: 6440475]
16. Hancock RE, Farmer SW. Mechanism of uptake of deglucoteicoplanin amide derivatives across outer membranes of *Escherichia coli* and *Pseudomonas aeruginosa*. Antimicrob Agents Chemother 1993;37:453–456. [PubMed: 8460914]
17. Ono S, Lee S, Kodera Y, Aoyagi H, Waki M, Kato T, Izumiya N. Environment-dependent conformation and antimicrobial activity of a gramicidin S analog containing leucine and lysine residues. FEBS Lett 1987;220:332–336. [PubMed: 2440729]

NIH-PA Author Manuscript

NIH-PA Author Manuscript

NIH-PA Author Manuscript

18. Hancock RE, Wong PG. Compounds which increase the permeability of the *Pseudomonas aeruginosa* outer membrane. Antimicrob Agents Chemother 1984;26:48–52. [PubMed: 6433788]
19. Wu M, Maier E, Benz R, Hancock RE. Mechanism of interaction of different classes of cationic antimicrobial peptides with planar bilayers and with the cytoplasmic membrane of *Escherichia coli*. Biochemistry 1999;38:7235–7242. [PubMed: 10353835]
20. Sims PJ, Waggoner AS, Wang CH, Hoffman JF. Studies on the mechanism by which cyanine dyes measure membrane potential in red blood cells and phosphatidylcholine vesicles. Biochemistry 1974;13:3315–3330. [PubMed: 4842277]
21. McInnes C, Kondejewski LH, Hodges RS, Sykes BD. Development of the structural basis for antimicrobial and hemolytic activities of peptides based on gramicidin S and design of novel analogs using NMR spectroscopy. J Biol Chem 2000;275:14287–14294. [PubMed: 10799508]
22. Sreerama N, Manning MC, Powers ME, Zhang JX, Goldenberg DP, Woody RW. Tyrosine, phenylalanine, and disulfide contributions to the circular dichroism of proteins: circular dichroism spectra of wild-type and mutant bovine pancreatic trypsin inhibitor. Biochemistry 1999;38:10814–10822. [PubMed: 10451378]
23. Manning MC, Woody RW. Theoretical study of the contribution of aromatic side chains to the circular dichroism of basic bovine pancreatic trypsin inhibitor. Biochemistry 1989;28:8609–8613. [PubMed: 2481497]
24. Woody RW. Aromatic side-chain contributions to the far ultraviolet circular dichroism of peptides and proteins. Biopolymers 1978;17:1451–1467.
25. Sereda TJ, Mant CT, Sonnichsen FD, Hodges RS. Reversed-phase chromatography of synthetic amphipathic alpha-helical peptides as a model for ligand/receptor interactions. Effect of changing hydrophobic environment on the relative hydrophilicity/hydrophobicity of amino acid side-chains. J Chromatogr A 1994;676:139–153. [PubMed: 7921171]
26. Yamagami C, Haraguchi M. Hydrophobicity parameters determined by reversed-phase liquid chromatography. XIV Application of a new hydrogen-accepting scale of monosubstituted pyrazines to analysis of the relationship between octanol-water partition coefficients and retention factors measured in different mobile phases. Chem Pharm Bull (Tokyo) 2000;48:1973–1977. [PubMed: 11145153]
27. Bull HB, Breese K. Surface tension of amino acid solutions: a hydrophobicity scale of the amino acid residues. Arch Biochem Biophys 1974;161:665–670. [PubMed: 4839053]
28. Nozaki Y, Tanford C. The solubility of amino acids and two glycine peptides in aqueous ethanol and dioxane solutions. Establishment of a hydrophobicity scale. J Biol Chem 1971;246:2211–2217. [PubMed: 5555568]
29. Prenner EJ, Lewis RN, Jelokhani-Niaraki M, Hodges RS, McElhaney RN. Cholesterol attenuates the interaction of the antimicrobial peptide gramicidin S with phospholipid bilayer membranes. Biochim. Biophys. Acta 2001;1510:83–92. [PubMed: 11342149]
30. Lewis RN, Kiricsi M, Prenner EJ, Hodges RS, McElhaney RN. Fourier transform infrared spectroscopic study of the interactions of a strongly antimicrobial but weakly hemolytic analogue of gramicidin S with lipid micelles and lipid bilayer membranes. Biochemistry 2003;42:440–449. [PubMed: 12525171]
31. Kondejewski LH, Lee DL, Jelokhani-Niaraki M, Farmer SW, Hancock RE, Hodges RS. Optimization of microbial specificity in cyclic peptides by modulation of hydrophobicity within a defined structural framework. J Biol Chem 2002;277:67–74. [PubMed: 11682479]
32. Wieprecht T, Dathe M, Beyermann M, Krause E, Maloy WL, MacDonald DL, Bienert M. Peptide hydrophobicity controls the activity and selectivity of magainin 2 amide in interaction with membranes. Biochemistry 1997;36:6124–6132. [PubMed: 9166783]
33. Liu LP, Deber CM. Guidelines for membrane protein engineering derived from *de novo* designed model peptides. Biopolymers 1998;47:41–62. [PubMed: 9692326]
34. Tossi A, Sandri L, Giangaspero A. Amphipathic, alpha-helical antimicrobial peptides. Biopolymers 2000;55:4–30. [PubMed: 10931439]
35. Houston ME Jr, Kondejewski LH, Karunaratne DN, Gough M, Fidai S, Hodges RS, Hancock RE. Influence of preformed alpha-helix and alpha-helix induction on the activity of cationic antimicrobial peptides. J Pept Res 1998;52:81–88. [PubMed: 9727863]

NIH-PA Author Manuscript

NIH-PA Author Manuscript

NIH-PA Author Manuscript

36. Shai Y, Oren Z. Diastereoisomers of cytolysins, a novel class of potent antibacterial peptides. J Biol Chem 1996;271:7305–7308. [PubMed: 8631748]

37. Oren Z, Shai Y. Selective lysis of bacteria but not mammalian cells by diastereomers of melittin: structure-function study. Biochemistry 1997;36:1826–1835. [PubMed: 9048567]

38. Krause E, Beyermann M, Dathe M, Rothemund S, Bienert M. Location of an amphipathic alpha-helix in peptides using reversed-phase HPLC retention behavior of D-amino acid analogs. Anal Chem 1995;67:252–258. [PubMed: 7856879]

39. Prenner EJ, Lewis RN, McElhaney RN. The interaction of the antimicrobial peptide gramicidin S with lipid bilayer model and biological membranes. Biochim. Biophys. Acta 1999;1462:201–221. [PubMed: 10590309]

40. Prenner EJ, Lewis RN, Kondejewski LH, Hodges RS, McElhaney RN. Differential scanning calorimetric study of the effect of the antimicrobial peptide gramicidin S on the thermotropic phase behavior of phosphatidylcholine, phosphatidylethanolamine and phosphatidylglycerol lipid bilayer membranes. Biochim. Biophys. Acta 1999;1417:211–223. [PubMed: 10082797]

41. Staudegger E, Prenner EJ, Kriechbaum M, Degovics G, Lewis RN, McElhaney RN, Lohner K. X-ray studies on the interaction of the antimicrobial peptide gramicidin S with microbial lipid extracts: evidence for cubic phase formation. Biochim. Biophys. Acta 2000;1468:213–230. [PubMed: 11018666]

42. Salgado J, Grage SL, Kondejewski LH, Hodges RS, McElhaney RN, Ulrich AS. Membrane-bound structure and alignment of the antimicrobial beta-sheet peptide gramicidin S derived from angular and distance constraints by solid state ^{19}F-NMR. J Biomol NMR 2001;21:191–208. [PubMed: 11775737]

NIH-PA Author Manuscript

NIH-PA Author Manuscript

NIH-PA Author Manuscript

Peptide Name	Sequence
GS14X$_L$4 series	**2 4 6 8 10 12 14**
GS14	cyclo -VKLKV***Y***PLKVKL***Y***P
GS14L$_L$4	cyclo ----L----------
GS14F$_L$4	cyclo ----F----------
GS14Y$_L$4	cyclo ----Y----------
GS14N$_L$4	cyclo ----N----------
GS14X$_D$4 series	
GS14K$_D$4	cyclo ----***K***----------
GS14L$_D$4	cyclo ----***L***----------
GS14F$_D$4	cyclo ----***F***----------
GS14Y$_D$4	cyclo ----***Y***----------
GS14N$_D$4	cyclo ----***N***----------
GS14G4	cyclo ----G----------

Figure 1.

Sequences of GS14X4 peptides used in this study, where X is the amino acid substituted at position 4, and the subscript L or D denotes the stereochemistry. One-letter amino acid code is used; bold italicized letters denote D-amino acids. The peptides are cyclized between the α-NH_2 and α-COOH groups.

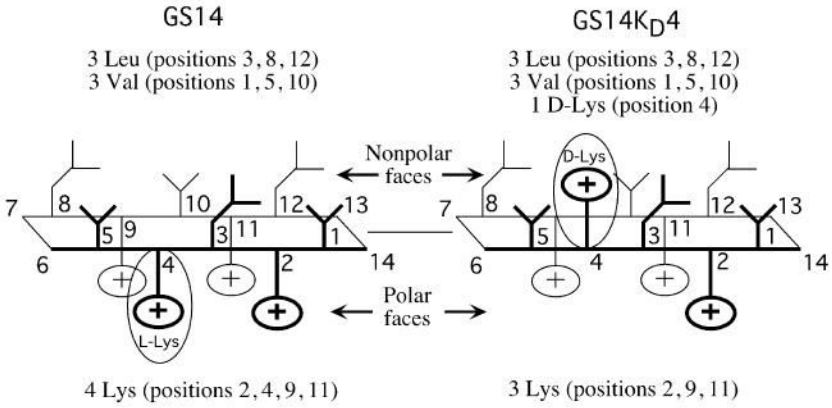

Figure 2.

Representations of GS14X4 analogs. L-amino acid side-chains at position 4 in GS14X$_l$4 peptides project onto the polar face (left panel), while D-amino acid side-chains at position 4 in GS14X$_d$4 peptides project onto the nonpolar face (right panel). The bold portions of the molecule denote proximity to the viewer. Examples shown are GS14 (left) and GS14K$_d$4 (right). Amino acids are numbered clockwise around the ring (see Fig. 1 for complete sequences).

NIH-PA Author Manuscript NIH-PA Author Manuscript NIH-PA Author Manuscript

NIH-PA Author Manuscript

NIH-PA Author Manuscript

NIH-PA Author Manuscript

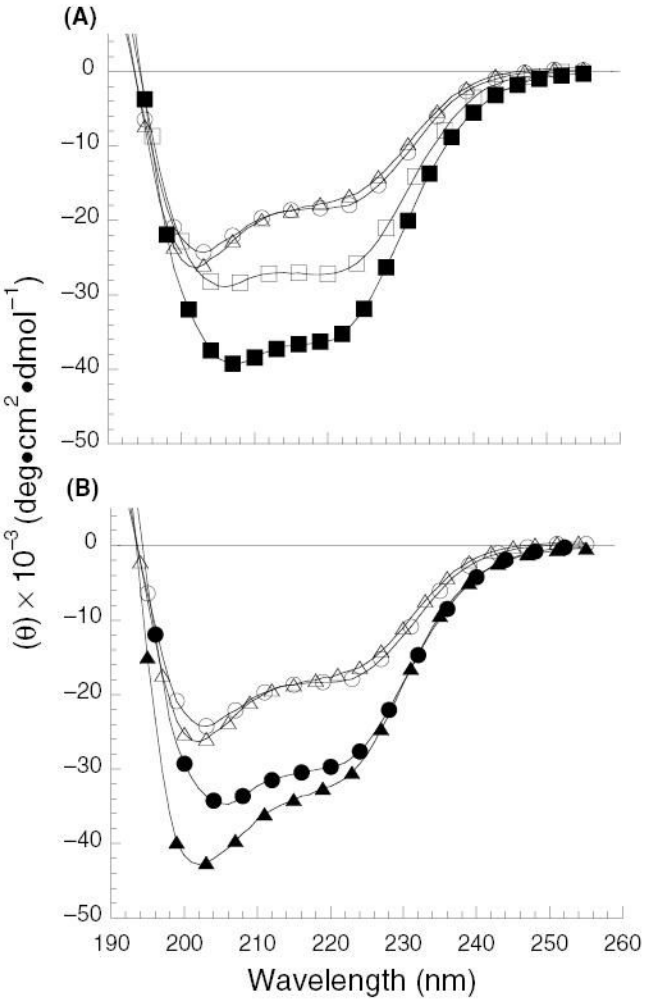

Figure 3.

Representative circular dichroism spectra of GS14X4 peptides. Panel A: peptides with D-Leu (open triangles), Gly (open circles) and L-Leu (open squares) substituted at position 4 in benign buffer (5 mM sodium acetate, pH 5.5, at 20 °C). Closed squares denote the L-Leu peptide in 5 mM sodium acetate, pH 5.5 at 20 °C, 50% trifluoroethanol. Panel B: peptides in the presence (closed symbols) and absence (open symbols) of 50% TFE.

NIH-PA Author Manuscript

NIH-PA Author Manuscript

NIH-PA Author Manuscript

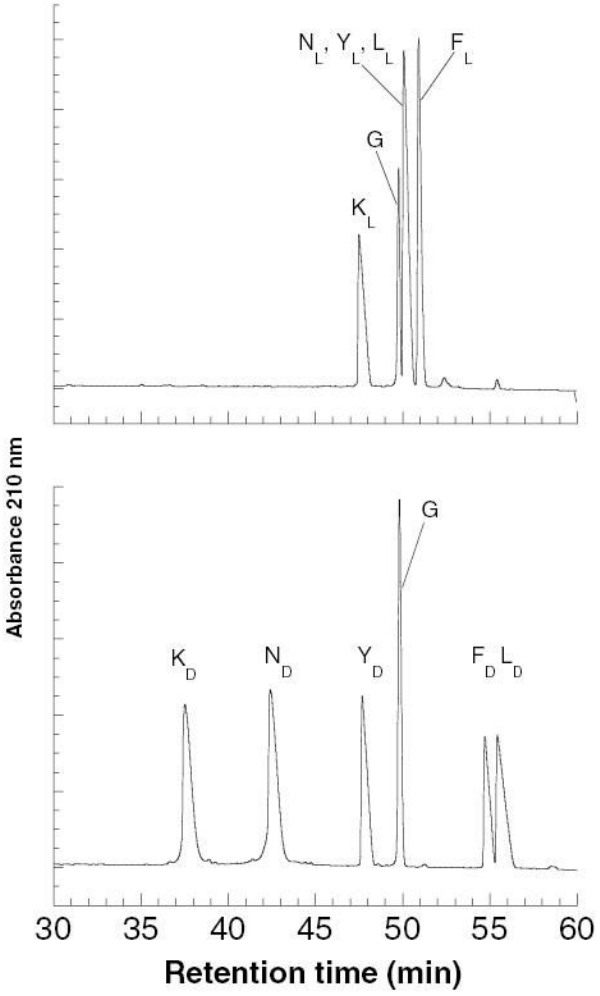

Figure 4.

Reversed-phase HPLC separation of the 14-residue cyclic peptides with L-amino substitutions at position 4 (X_l, top panel) and D-amino acid substitutions at position 4 (X_D, lower panel). One-letter code is used to denote the amino acid substitution, with the subscript L or D indicating the side-chain stereochemistry.

NIH-PA Author Manuscript

NIH-PA Author Manuscript

NIH-PA Author Manuscript

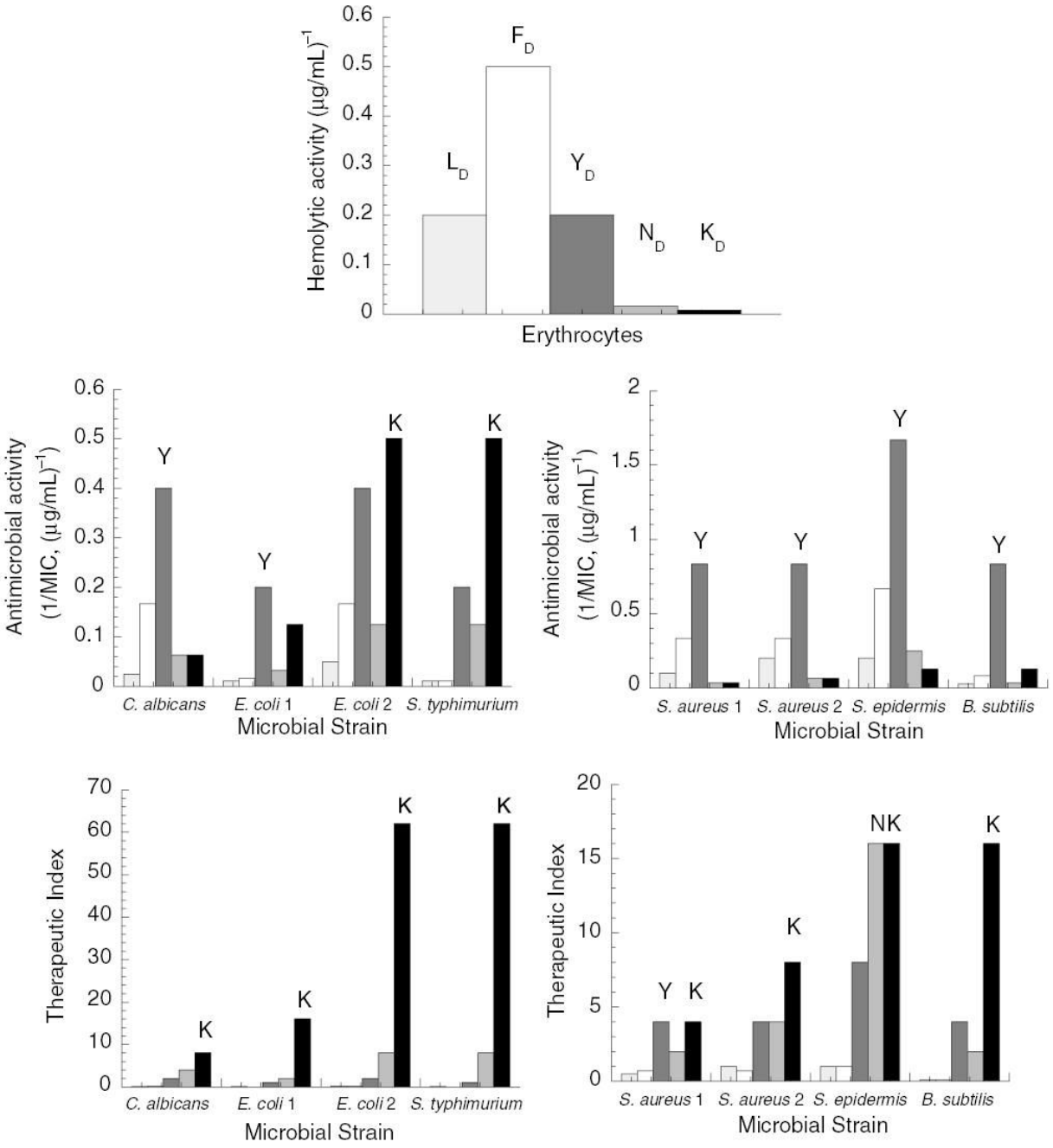

Figure 5.

Biologic activity of GS14X_d4 peptides. Top panel: hemolytic activity of peptides substituted with D-amino acids, plotted in reciprocal units, $(\mu g/mL)^{-1}$. Peptides were displayed from left to right in the order of decreasing overall hydrophobicity (L_d, F_d, Y_d, N_d, K_d) as follows: light grey, GS14L_d4; open box, GS14F_d4; dark grey box, GS14Y_d4; medium grey, GS14N_d4; black box, GS14K_d4. Second and third panels, antimicrobial activity of GS14X_d4 peptides against yeast and gram-negative and gram-positive bacteria, plotted in reciprocal units, $(\mu g/mL)^{-1}$. Fourth and fifth panels, therapeutic index (TI) of GS14X_d4 peptides against yeast and gram-negative and gram-positive bacteria. Higher values in the graphs indicate stronger hemolytic activity, more potent antimicrobial activity, and a higher TI. Microbial strains were the same

NIH-PA Author Manuscript

NIH-PA Author Manuscript

NIH-PA Author Manuscript

as those reported in Tables 3 and 4. Peptides with L-amino acids or Gly substituted at position 4 displayed strong hemolytic activity and poor antimicrobial activity, resulting in a low therapeutic index (<1), and were omitted from graphs (see Tables 3 and 4 for activity values).

NIH-PA Author Manuscript

NIH-PA Author Manuscript

NIH-PA Author Manuscript

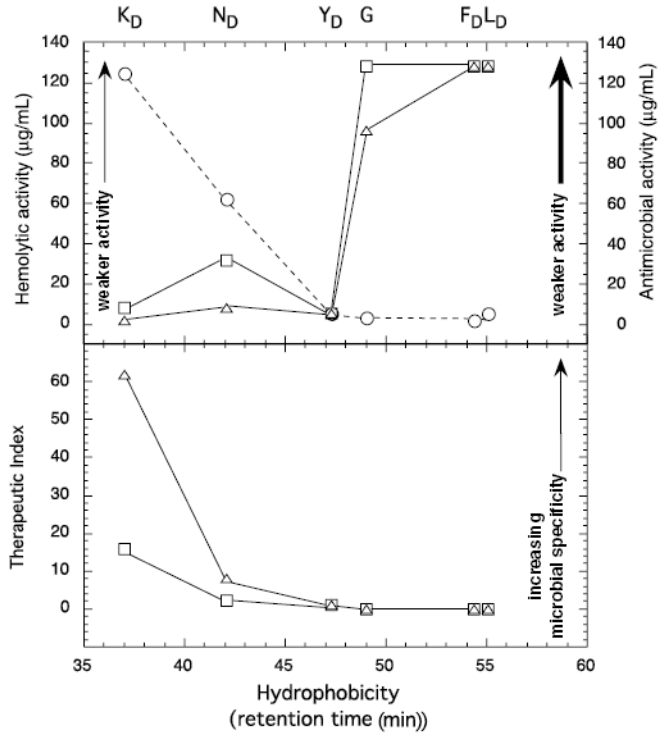

Figure 6.

Comparison of biologic activity and hydrophobicity of GS14-X_d4 peptides. Upper panel: hemolytic activity against human erythrocytes (dashed line) and antimicrobial activity (solid line) against *Escherichia coli* UB1005 (open squares) and *Salmonella typhimurium* C610 (open triangles) were plotted vs. reversed-phase HPLC retention times of the peptide analogs. Amino acid substitutions at position 4 are listed above their respective peptide retention times. One letter codes are used, with the subscript D denoting side-chain stereochemistry. Lower panel: therapeutic index (hemolytic activity/antimicrobial activity) of GS14X4 peptides for *E. coli* UB1005 and *S. typhimurium* C610.

NIH-PA Author Manuscript
NIH-PA Author Manuscript
NIH-PA Author Manuscript

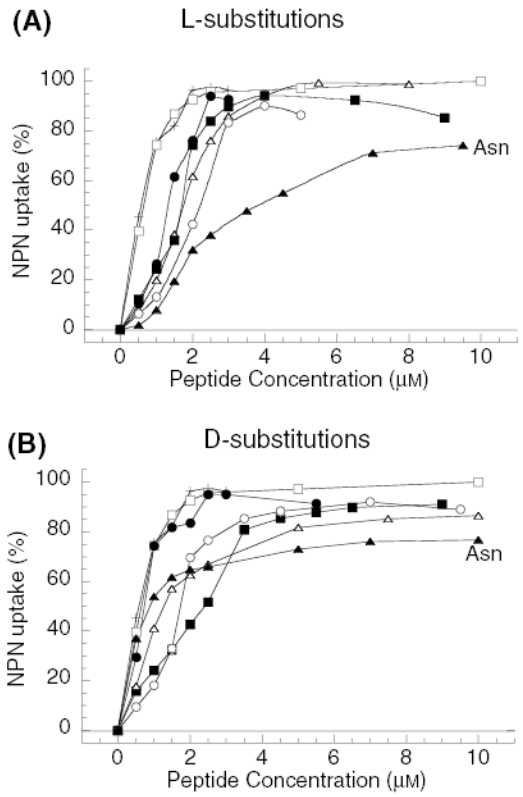

Figure 7.

Uptake of NPN in *Escherichia coli* outer membranes. Panel A: GS14X4 peptides substituted with L-amino acids at position 4, as well as the glycine-substituted peptide, GS14G4 (+) and polymyxin B (open square). Panel B: GS14X4 peptides substituted with D-amino acids at position 4, as well as the glycine-substituted peptide, GS14G4 (+) and polymyxin B (open square). Amino acids substitutions in both panels were L- (top panel) or D- (bottom panel) Lys (closed square), Leu (open circle), Phe (closed circle), Tyr (open triangle), and Asn (closed triangle).

NIH-PA Author Manuscript

NIH-PA Author Manuscript

NIH-PA Author Manuscript

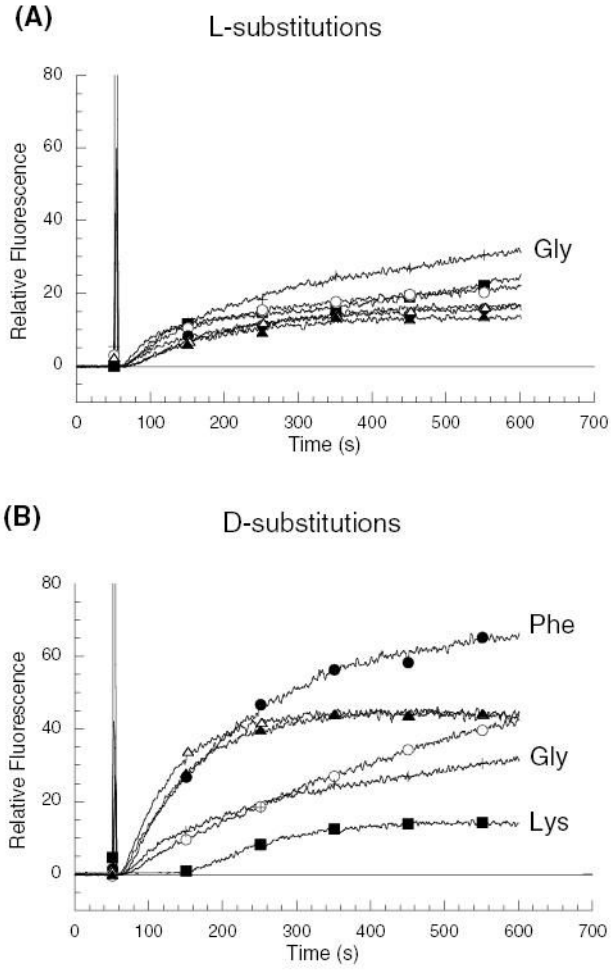

Figure 8.

Release of $diSC_3(5)$ from *Escherichia coli* cytoplasmic membranes by GS14X4 peptides. Panel A: dye release from peptides substituted with L-amino acids at position 4, as well as the glycine-substituted peptide, GS14G4 (+). Panel B: dye release from peptides substituted with D-amino acids at position 4 as well as the glycine-substituted peptide, GS14G4 (+). Addition of peptide is indicated by the spike in the plots at ~60 s. The peptides were incubated with cells at the MIC concentrations obtained for *E. coli* DC2 (Table 3). Amino acids substitutions in both panels were L- (top panel) or D- (bottom panel) Lys (closed square), Leu (open circle), Phe (closed circle), Tyr (open triangle), and Asn (closed triangle).

NIH-PA Author Manuscript

NIH-PA Author Manuscript

NIH-PA Author Manuscript

Table 1

Circular dichroism data for GS14 analogs

Substitution[a]	$[\theta]_{220}$ Benign[b]			$[\theta]_{220}$ 50% TFE[c]			$\Delta[\theta]_{220}$ TFE–benign[d]	
	L	D	Δ(L − D)	L	D	Δ(L − D)	L	D
Leu	−27 200	−17 600	−9600	−36 200	−32 300	−3900	−9000	−14 700
Phe	−26 200	−24 100	−2100	−36 100	−34 000	−2100	−9900	−9900
Tyr	−27 300	−23 000	−4300	−34 200	−29 900	−4300	−6900	−6900
Asn	−29 600	−11 200	−18 400	−37 300	−23 400	−13 900	−7700	−12 200
Lys	−26 300	−14 200	−12 100	−33 600	−27 800	−5800	−7300	−13 600
Gly	−18 400			−29 700			−11 300	

[a] Amino acid substitution at position 4 of GS14. Side-chain stereochemistry is denoted columns labeled L and D, with achiral Gly listed between L and D columns.

[b] Peptide mean residue molar ellipticity at 220 nm in benign medium (5 mM sodium acetate, pH 5.5, 20 °C). Δ(L − D) is the difference in mean residue molar ellipticity between the L-diastereomer and D-diastereomer.

[c] Peptide mean residue molar ellipticity at 220 nm in 50% trifluoroethanol, 5 mM sodium acetate, pH 5.5.

[d] Inducible structure, calculated as the difference between molar ellipticities at 220 nm for peptides in 50% TFE and benign conditions.

NIH-PA Author Manuscript

NIH-PA Author Manuscript

NIH-PA Author Manuscript

Table 2

HPLC retention times for GS14X4 peptides

Substitution[a]	t_r[b] (min)		$\Delta t_{r,Gly}$[c] (min)	
	L	D	L	D
Leu	49.8	55.1	0.8	6.1
Phe	50.2	54.4	1.2	5.4
Tyr	49.6	47.3	0.6	−1.7
Asn	49.7	42.1	0.7	−6.9
Lys	46.7	37.0	−2.3	−12.0
Gly	49.0		0.0	

[a] Amino acid substitution at position 4 of GS14. Side-chain stereochemistry is denoted columns labelled L and D, with achiral Gly listed in the L column.

[b] Peptide retention time from a reversed-phase HPLC column eluted at 1% acetonitrile/min (see Materials and Methods).

[c] Peptide RP-HPLC retention time relative to GS14G4 retention time, calculated as Δt_r (GS14X4) − t_r (GS14G4).

NIH-PA Author Manuscript NIH-PA Author Manuscript NIH-PA Author Manuscript

Table 3

Biologic activity of GS14 analogs against yeast and gram-negative bacteria

Substitution[a]	Hemolytic activity[b] (μg/mL)		*C. albicans*[c]					*E. coli* 1[c]					*E. coli* 2[c]					*S. typhimurium*[c]				
			MIC[d] (μg/mL)		Index[e]		Gain[f] (D/L)	MIC[d] (μg/mL)		Index[e]		Gain[f] (D/L)	MIC[d] (μg/mL)		Index[e]		Gain[f] (D/L)	MIC[d] (μg/mL)		Index[e]		Gain[f] (D/L)
	L	D	L	D	L	D		L	D	L	D		L	D	L	D		L	D	L	D	
Leu	3	5	90	40	0.03	0.1	3	>90	>80	0.02	0.04	2	45	20	0.06	0.2	3	>90	>80	0.02	0.04	2
Phe	3	2	>90	6	0.02	0.2	10	>90	>48	0.02	0.01	0.5	45	6	0.07	0.2	3	>90	>48	0.02	0.01	0.5
Tyr	8	5	>64	2.5	0.06	2	33	64	5	0.06	1	17	32	2.5	0.20	2	10	>64	5	0.06	1	17
Asn	2	62	>64	16	0.02	4	*200*	>64	32	0.02	2	100	32	8	0.06	8	133	>64	8	0.02	8	400
Lys	2	125	32	16	0.06	8	133	64	8	0.02	16	*800*	32	2	0.06	62	*1033*	32	2	0.06	62	*1033*
Gly	3		96		0.03		–	>96		0.02		–	48		0.06		–	96		0.03		–

[a] Amino acid substitution at position 4 of GS14. Side-chain stereochemistry is denoted columns labeled L and D, with achiral Gly listed in the L column.

[b] Minimal peptide concentration required for complete red blood cell lysis after 24 h at 37 °C (see Materials and Methods). The peptide showing the weakest hemolytic activity is italicized.

[c] Bacterial strain assayed. *C. albicans* is wild-type *Candida albicans; E. coli* 1 is wild-type *Escherichia coli* strain UB1005; *E. coli* 2 is antibiotic-sensitive strain DC2; *S. typhimurium* is antibiotic-sensitive *Salmonella typhimurium* strain C610.

[d] Minimal peptide concentration required to completely inhibit bacterial growth after 24 h. Peptides showing strong (<10 μg/mL) activity are italicized.

[e] Therapeutic index, calculated as hemolytic activity (μg/mL)/MIC (μg/mL). MIC values that exceeded the highest concentration tested were arbitrarily assigned the value 128 μg/mL for calculations.

[f] Gain or improvement in therapeutic index for GS14X$_D$4 over GS14X$_L$4 diastereomers. Gain is calculated as (therapeutic index, D-diastereomer)/(therapeutic index, L-diastereomer). The largest improvement in specificity of the D-peptide over the L-peptide is italicized.

J Pept Res. Author manuscript; available in PMC 2006 May 19.

NIH-PA Author Manuscript
NIH-PA Author Manuscript
NIH-PA Author Manuscript

Table 4

Biologic activity of GS14 analogs against gram-positive bacteria

Substitution[a]	Hemolytic activity[b] (μg/mL)		*S. aureus* 1[c]					*S. aureus* 2[c]					*S. epidermidis*[c]					*B. subtilis*[c]				
			MIC[d] (μg/mL)		Index[e]		Gain[f] (D/L)	MIC[d] (μg/mL)		Index[e]		Gain[f] (D/L)	MIC[d] (μg/mL)		Index[e]		Gain[f] (D/L)	MIC[d] (μg/mL)		Index[e]		Gain[f] (D/L)
	L	D	L	D	L	D		L	D	L	D		L	D	L	D		L	D	L	D	
Leu	3	5	45	10	0.1	0.6	6	11	*5*	0.2	1.2	6	22	*5*	0.1	1.2	12	90	40	0.03	0.1	3
Phe	3	2	45	*3*	0.1	0.7	7	11	*3*	0.3	0.7	2	45	*1.5*	0.1	1	10	90	12	0.03	0.1	3
Tyr	8	5	32	*1.2*	0.2	4	20	16	*1.2*	0.5	4	8	32	*0.6*	0.2	8	40	>64	*1.2*	0.10	4	40
Asn	2	62	32	32	0.1	2	20	16	16	0.1	4	40	16	*4*	0.1	16	*160*	>64	32	0.01	2	200
Lys	2	*125*	16	32	0.1	4	*40*	16	16	0.1	8	*80*	*8*	*8*	0.2	16	80	>64	8	0.01	16	*1600*
Gly	3		12		0.2		–	12		0.2		–	12		0.2		–	48		0.06		–

[a] Amino acid substitution at position 4 of GS14. Side-chain stereochemistry is denoted columns labeled L and D, with achiral Gly listed in the L column.

[b] Minimal peptide concentration required for complete red blood cell lysis after 24 h at 37 °C (see Materials and Methods). The peptide showing the weakest hemolytic activity is italicized.

[c] Bacterial strain assayed. *S. aureus* is wild-type *Staphylococcus aureus* strain 25923; *S. aureus* 2 is methicillin-resistant strain SAP0017; *S. epidermidis* is wild-type strain C621; *B. subtilis* is wild-type *Bacillus subtilis.*

[d] Minimal peptide concentration required to completely inhibit bacterial growth after 24 h. Peptides showing strong (<10 μg/mL) activity are italicized.

[e] Therapeutic index, calculated as hemolytic activity (μg/mL)/MIC (μg/mL). MIC values that exceeded the highest concentration tested were arbitrarily assigned the value 128 μg/mL for calculations.

[f] Gain or improvement in therapeutic index for GS14X$_D$4 over GS14X$_L$4 diastereomers. Gain is calculated as (therapeutic index, D-diastereomer)/(therapeutic index, L-diastereomer). The largest improvement in specificity of the D-peptide over the L-peptide is italicized.

J Pept Res. Author manuscript; available in PMC 2006 May 19.